

AperTO - Archivio Istituzionale Open Access dell'Università di Torino

**Erythropoietin administration partially prevents adipose tissue loss in experimental cancer cachexia models**

**This is the author's manuscript**

*Original Citation:*

*Availability:*

This version is available <http://hdl.handle.net/2318/144644> since 2016-01-17T21:44:04Z

*Published version:*

DOI:10.1194/jlr.M038406

*Terms of use:*

Open Access

Anyone can freely access the full text of works made available as "Open Access". Works made available under a Creative Commons license can be used according to the terms and conditions of said license. Use of all other works requires consent of the right holder (author or publisher) if not exempted from copyright protection by the applicable law.

(Article begins on next page)



# UNIVERSITÀ DEGLI STUDI DI TORINO

***This is an author version of the contribution published on:***

*Questa è la versione dell'autore dell'opera:*

*J Lipid Res. 2013 Nov;54(11):3045-51. doi: 10.1194/jlr.M038406.*

***The definitive version is available at:***

*La versione definitiva è disponibile alla URL:*

*<http://www.jlr.org/content/54/11/3045.abstract?sid=688e2980-1f15-4af3-89a9-8c58ed1b93c0>*

**ERYTHROPOIETIN ADMINISTRATION PARTIALLY PREVENTS  
ADIPOSE TISSUE LOSS IN EXPERIMENTAL CANCER CACHEXIA MODELS**

Fabio Penna<sup>1,3</sup>, Silvia Busquets<sup>1,2</sup>, Miriam Toledo<sup>1</sup>, Fabrizio Pin<sup>3</sup>, David Massa<sup>1</sup>,

Francisco J. López-Soriano<sup>1,2</sup>, Paola Costelli<sup>3</sup> and Josep M. Argilés<sup>1,2</sup>.

<sup>1</sup>Cancer Research Group, Departament de Bioquímica i Biologia Molecular,  
Facultat de Biologia, Universitat de Barcelona, Diagonal 643, Barcelona, Spain.

<sup>2</sup>Institut de Biomedicina de la Universitat de Barcelona (IBUB), Barcelona, Spain.

<sup>3</sup>Department of Clinical and Biological Sciences, University of Torino, Torino, Italy.

**Address for correspondence:**

\*Dra. Silvia Busquets, Cancer Research Group, Departament de Bioquímica i Biologia Molecular, Facultat de Biologia, Universitat de Barcelona, Diagonal 643, 08028-Barcelona, Spain. Telephone: 34-934034609 / telefax: 34-934021559 / e-mail: [silviabusquets@ub.edu](mailto:silviabusquets@ub.edu)

## ABSTRACT

Cancer-associated cachexia is characterized, among other symptoms, by a dramatic loss of both muscle and fat. In addition, the cachectic syndrome is often associated with anaemia. For this reason the object of the present investigation was to assess the effects of erythropoietin (EPO) treatment on experimental cancer-cachexia models. The results clearly show that, in addition to the improvement of the haematocrit, EPO treatment promoted a partial preservation of adipose tissue, while exerted negligible effects on muscle loss. The action of EPO reported here refers to both *in vivo* and *in vitro* studies. As for the former, administration of EPO to tumour-bearing animals resulted in a significant increase of lipoprotein lipase (LPL) activity in adipose tissue, suggesting that the treatment favoured triacylglycerol (TG) accumulation in the adipose tissue. The *in vitro* experiments, using both adipose tissue slices and 3T3-L1 adipocytes, suggest that EPO is able to increase the lipogenic rate through the activation of its specific receptor (EPOR) therefore suggesting that this metabolic pathway, in addition to TG uptake by LPL, may also contribute to the beneficial effects of EPO on fat preservation in cancer cachexia

**Keywords:** Cancer cachexia, anaemia, erythropoietin, adipose tissue, EPOR

## INTRODUCTION

Cancer patients frequently develop a condition of general wasting known as cachexia. This is a multifactorial syndrome that complicates patients' management, increases morbidity and mortality rates, reduces the tolerance to antineoplastic therapies, and results in poor quality of life(1). Cachexia is characterized by wasting of muscle and adipose tissue, anaemia, anorexia and perturbations of the hormonal homeostasis. It occurs in 54 to 70% of newly diagnosed cancer patients(2), worsening their prognosis and clinical management and accounting for about 25% of cancer deaths(3). The pathogenetic mechanisms underlying cachexia are complex and only partially identified, thereby effective therapeutic strategies are lacking.

Anaemia is a frequent feature of patients with cancer cachexia, contributing to weight loss, reduced exercise capacity, and altered energy homeostasis(4). The incidence of anaemia varies with tumour type and stage, and patient's age: up to one-third of cancer hosts are anaemic at diagnosis(5) and chemotherapy frequently increases this number. Cancer-associated anaemia can thus be considered a negative prognostic factor for survival(6). Anaemia can lead to hypoxia in several tissues, increasing lactate production and thereby promoting a decrease in intracellular pH that enhances muscle protein degradation, possibly exacerbating tissue wasting(7). Nevertheless, mechanistic data explaining how anaemia may contribute to the onset and progression of cachexia are still lacking.

Erythropoietin (EPO), a 34kDa glycoprotein, is synthesized by the kidney in response to hypoxemia. Its main function is to stimulate erythropoiesis by activating the EPO receptor (EPOR) on erythroid progenitor cells. EPO signals through phosphatidylinositol-3-kinase (PI3K)/Akt, signal transducer and activator of transcription 5 (STAT5), mitogen-activated protein kinase (MAPK) and protein kinase C pathways, inducing erythroblast production with a consequent rise in red blood cell count evident 1–2 weeks after EPO administration(8). EPO has been used for the treatment of cancer wasting to fight the anaemia associated with the cachectic syndrome. EPO treatment in unselected randomized cachectic cancer patients prevented the appearance of anaemia and the loss of exercise capacity, showing a trend to significant improvement in general health(9). It has also been used in combination with cyclooxygenase (COX) inhibitors(10). Moreover, in anaemic

cancer patients with non-myeloid malignancies, EPO treatment increased haemoglobin levels, decreased transfusion requirements, and improved both patients' functional status and quality of life(11).

Recently, the discovery that EPOR is expressed on skeletal myoblasts suggests that the role of EPO may extend beyond erythropoiesis. Such hypothesis is supported by observations showing that EPO enhances the proliferation and reduces the differentiation of both primary satellite cell cultures and C2C12 myoblasts(12). Moreover, intra-muscular EPO administration after crush injury of rat skeletal muscle induces a faster and better regeneration with improved microcirculation(13). Besides the skeletal muscle, also the adipose tissue, that is strongly affected during cachexia, has been recently suggested as target of EPO action(14). Indeed, EPO administration to nude mice previously transplanted with human fat tissue determined longer survival and stimulated the angiogenesis of the grafts, such effects being comparable to those exerted by the pro-angiogenic protein vascular endothelial growth factor (VEGF)(14).

Considering the possible contribution of EPO signalling in the maintenance of both muscle and adipose tissue homeostasis, the aim of the present investigation was to examine, beyond the correction of anaemia, the effects of EPO treatment on either skeletal muscle or adipose tissue during experimental cancer cachexia.

## MATERIALS AND METHODS

### Experimental tumour models

C57BL/6 and Balb/C mice weighing about 20 g (Interfauna, Barcelona, Spain) and Wistar rats weighing about 150 g (Interfauna, Barcelona, Spain) were maintained on a regular dark-light cycle (light from 08:00 to 20:00), with free access to food and water during the whole experimental period. They were cared for in compliance with the *Policy on Humane Care and Use of Laboratory Animals* (ILAR 2011). The Bioethical Committee of the University of Barcelona approved the experimental protocol. All animal manipulations were made in accordance with the European Community guidelines for the use of laboratory animals. The day of sacrifice, the animals were weighed and anaesthetized with an i.p. injection of ketamine/xylazine mixture (3:1) (Imalgene<sup>®</sup> and Rompun<sup>®</sup> respectively). Tissues were rapidly excised, weighed, and frozen in liquid nitrogen.

#### A. Colon26 carcinoma

Tumour-bearing mice were inoculated subcutaneously in the back with  $5 \times 10^5$  Colon26 carcinoma cells. Colon26 cells were maintained *in vitro* in Dulbecco's Modified Eagle's Medium (DMEM, Invitrogen) supplemented with 10% FBS, 100 U/ml penicillin, 100 µg/ml streptomycin, 100 µg/ml sodium pyruvate, 2 mM L-glutamine, at 37°C in a humidified atmosphere of 5% CO<sub>2</sub> in air. The day of tumour implantation the cells were trypsinized, re-suspended in sterile saline and subsequently implanted in the back of the animals at the concentration indicated above. Animals were randomized and divided into two groups, namely controls (C) and tumour bearers (C26). C26 were divided into two sub-groups: untreated and treated i.p. every three days with recombinant human EPO (100 IU, Calbiochem) adopting the same protocol of a previous work(14). Mice were sacrificed under anaesthesia 14 days after tumour implantation.

#### B. Lewis lung carcinoma

Mice received an intramuscular (hind leg) inoculum of  $5 \times 10^5$  Lewis lung carcinoma cells obtained from previous tumour hosts. The Lewis lung carcinoma is a cachexia-inducing, rapidly growing murine tumour composed by poorly differentiated cells, with a relatively short doubling time(15). Animals were randomized and divided into two groups, namely controls (C) and tumour



bearers (LLC). LLC were divided into two sub-groups: untreated and treated with EPO (100 IU) that was administered i.p. every three days. Mice were sacrificed under anaesthesia 14 days after tumour implantation.

### **C. AH-130 Yoshida ascites hepatoma**

Male rats received an intraperitoneal inoculum of  $10^8$  AH-130 Yoshida ascites hepatoma cells obtained from exponential tumours(16). On day 7 after tumour transplantation, the animals were sacrificed and the dorsal fat pads were excised for subsequent *ex vivo* experiments.

#### **Haematocrit**

Total blood was withdrawn from anaesthetized mice by cardiac puncture and collected in heparinized tubes. A drop was used to fill haematocrit capillary tubes that were centrifuged in a haematocrit centrifuge for 5 min at 800 x g. Haematocrit was calculated as percentage of packed cell volume of the total blood.

#### **Lipoprotein lipase activity**

White adipose tissue (WAT) samples were homogenized in a buffer containing 10mM Hepes, 1mM EDTA, 1mM DTT, 250mM Sucrose, 5U/ml Heparin, pH 7.5 and used in an assay system containing [ $^3$ H]triolein as substrate (17); [ $^3$ H]fatty acids released after a 30 min incubation period were extracted and quantified by the method of Nilsson-Ehle and Schotz (18).

#### ***EX vivo* lipogenic rate**

After dissection, WAT from control and AH-130 bearing rats was weighed and sliced into fragments of about 15-20 mg. 100 mg (4-5 pieces) were incubated in 4 ml Krebs-Henseleit buffer (pH 7.4) containing 2% fatty acid-free bovine serum albumin, 5 mM D-glucose and 0,1  $\mu$ Ci/ml [1- $^{14}$ C] acetate. Where indicated, the following substances were added: TNF (5 ng/ml), EPO (10U/ml) and insulin (4  $\mu$ g/ml). Tissue slices were incubated for 1 hour at 37°C in a shaking water bath under O<sub>2</sub>/CO<sub>2</sub> (19:1) flow. Lipogenic rate was calculated by measuring [1- $^{14}$ C] acetate incorporation into fatty acids in WAT pieces as previously described(19).

### **Ex vivo lipolytic rate**

The lipolytic rate was determined as previously described by López-Soriano et al. (20). After dissection, WAT from control and AH-130 bearing rats was weighed and sliced into pieces of about 15-20 mg. 100 mg (4-5 pieces) were incubated in 4 ml Krebs-Henseleit buffer (pH 7.4) containing 2% fatty acid-free bovine serum albumin and 5 mM D-glucose. Where indicated, the following substances were added: TNF (5 ng/ml), EPO (10U/ml), insulin (4 µg/ml) and isoproterenol (0.5 µM). Tissue slices were incubated for 1 hour at 37°C in a shaking water bath under O<sub>2</sub>/CO<sub>2</sub> (19:1) flow. Incubations were stopped by adding perchloric acid (final concentration 3%). Lipolytic rate was estimated as the glycerol released to the incubation medium measured by the method of Hohorst et al.(21).

### **Cell Culture and Adipocyte Differentiation**

3T3-L1 preadipocytes (ATCC) were grown in DMEM supplemented with 10% (v/v) foetal calf serum (Invitrogen), 25 mM HEPES pH 7.0, 1,000 U/ml penicillin, 1,000 U/ml streptomycin, and 25 µg/ml fungizone (BioWhittaker). To induce adipocyte differentiation, cells were grown for 2 days post confluence and then cultured in differentiation medium consisting of DMEM supplemented with 10% (v/v) foetal bovine serum (Invitrogen), 25 mM HEPES pH 7.0, 1,000 U/ml penicillin, 1,000 U/ml streptomycin, and 25 µg/ml fungizone, plus MDI (0.5 mM isobutylmethyl-xanthine, 1µM dexamethasone and 1 µg/ml insulin). After 48 h, MDI was replaced with insulin (1 µg/ml) and the medium changed every two days.

### **Immunofluorescence**

3T3-L1 monolayers at day 4 of differentiation were washed with PBS and fixed in acetone-methanol (1:1), rehydrated with PBS containing 0.1% Triton X-100 and probed with an anti-EPOR primary antibody (R&D Systems, Minneapolis, MN, USA). Detection was performed using a Cy3-conjugated goat IgG secondary antibody. Nuclei were stained with the Hoechst 33342 fluorochrome and the images captured in an epiilluminated fluorescence microscope (Leica,

Solms, Germany).

### **Oil Red O staining**

Lipid accumulation in differentiating (Day 4) 3T3-L1 cells was assessed by Oil Red O staining. Briefly, cells were fixed for 15' in 3% paraformaldehyde, rinsed three times in PBS and stained for 30' with the lipophilic dye Oil Red O (Sigma) dissolved in 65% isopropanol. Dye excess was washed away and the cells were dried completely. Lipids were extracted with an exan/isopropanol mixture (3:2) and the absorbance read at 490nm.

### **Cell growth curve**

3T3-L1preadipocytes were seeded in 12-wells plates at  $4 \times 10^3$  cells/sq cm in growth medium (see above). After 12 h (point zero) and every 24h (for 4 days) the cells were washed with PBS, fixed in 4% paraformaldehyde, stained with Crystal violet (0,1% in PBS), washed three times and dried completely. The dye was extracted with 10% acetic acid and the absorbance read at 590nm.

### **Western blotting**

Total proteins from WAT samples or 3T3-L1 monolayers were extracted in RIPA buffer (50 mM Tris-HCl pH 7.4, 150 mM NaCl, 1% NP40, 0.25% Na-deoxycholate, 1 mM PMSF) with freshly added protease and phosphatase inhibitor cocktails, sonicated and centrifuged at 3000 x g for 5 min at 4°C, and the supernatant collected. Protein concentration was assayed by the method of Lowry (22) using BSA as working standard. Equal amounts of protein (30 µg) were heat-denatured in sample-loading buffer (50 mM Tris-HCl, pH 6.8, 100 mM DTT, 2% SDS, 0.1% bromophenol blue, 10% glycerol), resolved by SDS-PAGE and transferred to nitrocellulose membranes. The filters were blocked with Tris-buffered saline (TBS) containing 0.05% Tween and 5% non-fat dry milk and then incubated overnight with antibodies directed against: EPOR (R&D systems, Minneapolis, MN, USA), phosphorylated Akt (Cell Signalling, Beverly, MA, USA), total Akt (SantaCruz Biotechnology, Santa Cruz, CA, USA). Peroxidase-conjugated IgG (Bio-Rad, Hercules, CA, USA) were used as secondary antibodies. Membrane-bound immune complexes were detected by an enhanced chemiluminescence system (SantaCruz Biotechnology) on a photon-

sensitive film. Protein loading was normalized according to GAPDH (SantaCruz Biotechnology) expression. Band quantification was performed by densitometric analysis using a specific software (TotalLab, NonLinear Dynamics, Newcastle upon Tyne, UK).

### Real time-PCR

Total RNA was obtained using the TriPure reagent (Roche) following manufacturer's instructions. RNA concentration was determined fluorometrically using the Ribogreen reagent (Invitrogen). Total mRNA was retro-transcribed using the i-Script cDNA synthesis kit (Bio-Rad). Transcript levels were determined by using the SsoFast Evagreen Supermix and the MiniOpticon thermal cycler (Bio-Rad), normalizing the expression for both actin and calnexin levels. Primer sequences were as follows:

PPAR $\gamma$	CGGAAGCCCTTTGGTGACTT	
TGGGCTTCACGTTTCAGCAAG,	aP2	CAGAAGTGGGATGGAAAGTCG
CGACTGACTATTGTAGTGTTTGA,	SREBP-1c	GATGTGCGAACTGGACACAG
CATAGGGGGCGTCAAACAG,	FASN	TCCACCTTTAAGTTGCCCTG
TCTGCTCTCGTCATGTCACC, LPL	TCTGTACGGCACAGTGG	CCTCTCGATGACGAAGC, actin
CTGGCTCCTAGCACCATGAAGAT	GGTGGACAGTGAGGCCAGGAT,	calnexin
GCAGCGACCTATGATTGACAACC	GCTCCAAACCAATAGCACTGAAAGG.	

### Statistical Analysis

Data were analyzed by ANOVA. Statistical significance of results is indicated by: \*p < 0.05, \*\*p < 0.01, \*\*\*p < 0.001.

## RESULTS AND DISCUSSION

Cambiare numerazione figure, discutere protezione della metabolic capacity (Lundholm 1998, Daneryd 2002)!

In order to study the effects of EPO on tumour-induced wasting, we used two different murine experimental models: the Colon26 carcinoma (C26) and the Lewis lung carcinoma (LLC). As expected, tumour growth in both animal models resulted in important changes in body weight (Table 1; C26 -22%; LLC -22%) as well as in muscle (C26: GSN -23%, Tibialis -25%; LLC: GSN -29%, Tibialis -32%) and white adipose tissue (WAT) mass (C26: dorsal WAT -85%, epididimal WAT -77%; LLC: dorsal WAT -95%, epididimal WAT -87%). In both models, tumour-bearing mice showed reduced haematocrit; such effect was more evident in the LLC (-56%) than in the C26 hosts (-16%). EPO treatment did not modify either body or muscle weights in any of the groups. By contrast, in the C26-bearing animals EPO administration significantly increased both dorsal and epididimal WAT (+108% and +73%, respectively; Table 1A) as compared to the untreated tumour-bearing mice. Similar, but quantitatively more marked, results were found in the LLC-bearing mice (dorsal WAT: +200%, epididimal WAT: +112%; Table 1B). Finally, EPO treatment resulted in significant haematocrit rescue in both tumour-bearing groups (C26 +12%; LLC +20%), in the latter case not sufficient to re-establish the control levels. Food intake non cambia, quindi la protezione non dipende da maggiore calorie intake, mentre non siamo in grado di stabilire eventuali differenze di energy expenditure.

The results obtained in the LLC-bearing mice administered EPO, i.e. a relevant rescue of adipose tissue loss despite a small and far from complete rescue of anaemia prompted us to investigate the specific action of EPO in this tissue. The first step in order to define a direct rather than indirect action of the cytokine in the WAT was to assess the presence of the specific EPO receptor in the tissue. The results presented in Figure 1 clearly show that the receptor is expressed in the adipose tissue of both control and tumour-bearing mice at similar levels; moreover, EPO administration stimulated EPOR accumulation (+84%) in LLC-bearing mice. Such data are in agreement with the protective effects (Table 1) reported on WAT and point to a direct role of EPO

regulated signalling in the control of adipose tissue mass. Such a hypothesis is consistent with recent observations that reported the functional expression of EPOR in human adipose tissue(14). EPO effects are mediated by EPOR that transmits the intracellular signal mainly through the JAK-STATS or the PI3K-Akt pathways. Since the latter signalling pathway regulates adipocyte growth and anabolism, we measured the levels of total and phosphorylated Akt, a serine-threonine kinase downstream of PI3K. The results presented in Figure 2 show that the implantation of LLC led to a decrease of phosphorylated Akt, in agreement with decreased anabolic processes in the WAT of tumour-bearing animals. Treatment with EPO was able to partially prevent such a reduction, suggesting that the protective effects of EPO on adipose tissue against cancer cachexia are partially mediated through this intracellular signalling pathway (Figure 2).

To clarify the mechanisms underlying EPO-induced improvement of WAT depletion in tumour-bearing animals, the different pathways associated with fat accumulation have been investigated. Fatty acids (FA) enter adipose tissue through the action of lipoprotein lipase (LPL) on either VLDL (endogenous triacylglycerol) or chylomicra (exogenous triacylglycerol). This enzyme, located in the endothelial cells, breaks down triacylglycerol (TAG) into FA and glycerol. The FA can then be esterified and incorporated into tissue TAG. Total LPL activity is markedly reduced in mice bearing the LLC tumour (Figure 3). This observation is in agreement with previous results from our laboratory(23). Treatment with EPO significantly increases total LPL activity in tumour-bearing mice, although it still remains lower than control values. These data agree with the results obtained by Goto and co-workers in haemodialysis patients(24).

In addition to the entry of FA into adipose tissue through LPL, FA can also be synthesized *de novo* through lipogenesis inside the adipose tissue. For this reason, the effects of EPO on the lipogenic rate were investigated by measuring the incorporation into lipids of [1-<sup>14</sup>C]-acetate in rat WAT slices incubated in the presence of different stimuli. Figure 4A shows the rates of lipogenesis in different conditions. As expected, the lipogenic rate is markedly induced by insulin and significantly reduced by incubation of WAT slices with tumour necrosis factor alpha (TNF). Interestingly, while EPO alone had no significant lipogenic effects, it is able to abrogate TNF

effects. In the attempt to compare experimental cachexia with direct TNF effects on lipogenesis, a rat cachexia model (AH-130 Yoshida ascites hepatoma) was used. As expected, the lipogenic rate in WAT slices from tumour-bearing rats was markedly reduced. Of interest, such reduction was significantly improved (+130%) by the addition of EPO in the incubation medium. These results suggest that, in addition to LPL, lipogenesis also contributes to fat accretion observed as a result of EPO treatment in cachectic tumour-bearing animals.

Finally, the effects of EPO on adipose tissue could rely on decreased lipolytic rate. In order to test this hypothesis, we measured the glycerol release in WAT slices from control and AH-130-bearing rats in the presence of EPO. The results presented in Figure 4B show that both isoproterenol and TNF increased the rate of glycerol release (+34% and +274%, respectively), while insulin, as expected, exerted an opposite effect (-43%). Unexpectedly, the glycerol release from AH-130 samples was lower than the respective controls, such effect likely depending on the smaller amount of lipids present in the tissue of the former ones. No effects of EPO were observed on lipolysis in WAT from either control or tumour-bearing animals and from both TNF and isoproterenol treated samples, therefore excluding any EPO action on the regulation of lipolysis.

The effects exerted by EPO on the adipose tissue have been further investigated at the molecular level taking advantage of an *in vitro* model system, namely the 3T3-L1 pre-adipocytes, that can be induced to adipocyte differentiation when cultured in appropriate conditions (see Materials and methods). As shown in Figure 5, EPO administration to differentiating cells resulted in increased accumulation of lipid droplets as observed by both morphological appearance and quantification of Oil red O uptake. Such effect is associated with increased EPOR staining. In agreement with the above reported *ex vivo* results using WAT slices (Figure 4), the addition of TNF to the culture medium decreased lipid accumulation, an effect that was prevented by EPO. PCR che conferma *in vitro* i dati ottenuti *in vivo* dimostrando che EPO è in grado di attivare direttamente l'adipogenesi e di contrastare, almeno in parte, l'inibizione imposta dal TNF. The EPOR expression was then evaluated in a time-course experiment, from growing to fully differentiated cells. Figure 6A shows that the presence of EPO increased the receptor expression in growing cells and prolonged

the expression during the early phases of differentiation while then rapidly disappeared. These data suggest that EPO exerts its effects on the adipose tissue mainly targeting proliferating and differentiating pre-adipocytes though not fully differentiated adipocytes. On this line, a growth curve of pre-adipocytes was performed in order to clarify if EPO action might rely on adipocyte hyperplasia rather than hypertrophy. The results showed that EPO administration did not affect the cell proliferation rate (Figure 6B), clarifying that EPO is mainly responsible for the induction of lipogenesis and doesn't impinge on cell growth.

The results shown in the present study are consistent with a beneficial effect of EPO treatment on the preservation of adipose tissue wasting associated with cancer. Indeed, fat loss during cancer is a common trend both in humans and experimental models (25). As a consequence, some authors indicated that fat loss is associated with both poor prognosis and reduced survival during cancer (26). By contrast, no effects of EPO were observed in the preservation of skeletal muscle mass. These results are in contrast with a recent publication suggesting that preservation of adipose tissue during cachexia resulted in preservation of muscle mass, as if the muscle wasting was directly associated with the loss of adipose tissue(27). Concerning the metabolic pathways involved in the actions of EPO on fat mass, the results presented here clearly suggested that the cytokine acts on both lipogenesis and LPL-mediated uptake of circulating TAG (Figure 7).

In conclusion, EPO administration to cancer patients might be useful to counteract anaemia, often present in cancer cachexia, but also to preserve adipose tissue homeostasis and fat stores. Moreover, in the last few years adipose tissue has been recognised as an "endocrine tissue", due to the several cytokines and hormones released by adipocytes, thus highlighting the importance of its preservation in the design of future cancer cachexia treatments. Further studies are needed in order to better clarify the mechanisms of EPO action in non-hematopoietic cells. Furthermore, recent data showing that functional EPOR is absent in several human tumour cell lines(28) reduce the concerns regarding EPO safety for future clinical trials.



## **ACKNOWLEDGEMENTS**

This work was supported by a grant from the Ministerio de Ciencia y Tecnología (SAF2011-26091). FP was an AIRC/Marie Curie fellow in cancer research when the study was performed.

## REFERENCES

1. Muscaritoli, M., S. D. Anker, J. Argilés, Z. Aversa, J. M. Bauer, G. Biolo, Y. Boirie, I. Bosaeus, T. Cederholm, P. Costelli, K. C. Fearon, A. Laviano, M. Maggio, F. Rossi Fanelli, S. M. Schneider, A. Schols, and C. C. Sieber. 2010. Consensus definition of sarcopenia, cachexia and pre-cachexia: joint document elaborated by Special Interest Groups (SIG) "cachexia-anorexia in chronic wasting diseases" and "nutrition in geriatrics". *Clin Nutr* **29**: 154-159.
2. Muscaritoli, M., M. Bossola, Z. Aversa, R. Bellantone, and F. Rossi Fanelli. 2006. Prevention and treatment of cancer cachexia: new insights into an old problem. *Eur J Cancer* **42**: 31-41.
3. Loberg, R. D., D. A. Bradley, S. A. Tomlins, A. M. Chinnaiyan, and K. J. Pienta. 2007. The lethal phenotype of cancer: the molecular basis of death due to malignancy. *CA Cancer J Clin* **57**: 225-241.
4. Bruera, E., and C. Sweeney. 2000. Cachexia and asthenia in cancer patients. *Lancet Oncol* **1**: 138-147.
5. Knight, K., S. Wade, and L. Balducci. 2004. Prevalence and outcomes of anemia in cancer: a systematic review of the literature. *Am J Med* **116 Suppl 7A**: 11S-26S.
6. Caro, J. J., M. Salas, A. Ward, and G. Goss. 2001. Anemia as an independent prognostic factor for survival in patients with cancer: a systemic, quantitative review. *Cancer* **91**: 2214-2221.
7. Drochioiu, G. 2008. Chronic metabolic acidosis may be the cause of cachexia: body fluid pH correction may be an effective therapy. *Med Hypotheses* **70**: 1167-1173.
8. Jelkmann, W. 2007. Erythropoietin after a century of research: younger than ever. *Eur J Haematol* **78**: 183-205.
9. Lindholm, E., P. Daneryd, U. Korner, A. Hyltander, M. Fouladiun, and K. Lundholm. 2004. Effects of recombinant erythropoietin in palliative treatment of unselected cancer patients. *Clin Cancer Res* **10**: 6855-6864.
10. Lundholm, K., P. Daneryd, I. Bosaeus, U. Körner, and E. Lindholm. 2004. Palliative nutritional intervention in addition to cyclooxygenase and erythropoietin treatment for patients with malignant disease: Effects on survival, metabolism, and function. *Cancer* **100**: 1967-1977.
11. Shasha, D., M. J. George, and L. B. Harrison. 2003. Once-weekly dosing of epoetin-alpha increases hemoglobin and improves quality of life in anemic cancer patients receiving radiation therapy either concomitantly or sequentially with chemotherapy. *Cancer* **98**: 1072-1079.
12. Ogilvie, M., X. Yu, V. Nicolas-Metral, S. M. Pulido, C. Liu, U. T. Ruegg, and C. T. Noguchi. 2000. Erythropoietin stimulates proliferation and interferes with differentiation of myoblasts. *J Biol Chem* **275**: 39754-39761.
13. Rotter, R., M. Menshykova, T. Winkler, G. Matziolis, I. Stratos, M. Schoen, T. Bittorf, T. Mittlmeier, and B. Vollmar. 2008. Erythropoietin improves functional and histological recovery of traumatized skeletal muscle tissue. *J Orthop Res* **26**: 1618-1626.

14. Hamed, S., D. Egozi, D. Kruchevsky, L. Teot, A. Gilhar, and Y. Ullmann. 2010. Erythropoietin improves the survival of fat tissue after its transplantation in nude mice. *PLoS One* **5**: e13986.
15. Lippman, M. M., W. R. Laster, B. J. Abbott, J. Venditti, and M. Baratta. 1975. Antitumor activity of macromycin B (NSC 170105) against murine leukemias, melanoma, and lung carcinoma. *Cancer Res* **35**: 939-945.
16. Tessitore, L., P. Costelli, G. Bonetti, and F. M. Baccino. 1993. Cancer cachexia, malnutrition, and tissue protein turnover in experimental animals. *Arch Biochem Biophys* **306**: 52-58.
17. Ramirez, I., A. J. Kryski, O. Ben-Zeev, M. C. Schotz, and D. L. Severson. 1985. Characterization of triacylglycerol hydrolase activities in isolated myocardial cells from rat heart. *Biochem J* **232**: 229-236.
18. Nilsson-Ehle, P., and M. C. Schotz. 1976. A stable, radioactive substrate emulsion for assay of lipoprotein lipase. *J Lipid Res* **17**: 536-541.
19. Lopez-Soriano, J., J. M. Argiles, and F. J. Lopez-Soriano. 1995. Metabolic effects of tumour necrosis factor-alpha on rat brown adipose tissue. *Mol Cell Biochem* **143**: 113-118.
20. Lopez-Soriano, J., F. J. Lopez-Soriano, G. J. Bagby, D. H. Williamson, and J. M. Argiles. 1997. Anti-TNF treatment does not reverse the abnormalities in lipid metabolism of the obese Zucker rat. *Am J Physiol* **272**: E656-660.
21. Hohorst, H. J., F. H. Kreutz, and T. Buecher. 1959. [On the metabolite content and the metabolite concentration in the liver of the rat]. *Biochem Z* **332**: 18-46.
22. Lowry, O. H., N. J. Rosebrough, A. L. Farr, and R. J. Randall. 1951. Protein measurement with the Folin phenol reagent. *J Biol Chem* **193**: 265-275.
23. López-Soriano, J., J. M. Argilés, and F. J. López-Soriano. 1997. Sequential changes in lipoprotein lipase activity and lipaemia induced by the Yoshida AH-130 ascites hepatoma in rats. *Cancer Lett* **116**: 159-165.
24. Goto, T., H. Saika, T. Takahashi, A. Maeda, M. Mune, and S. Yukawa. 1999. Erythropoietin supplement increases plasma lipoprotein lipase and hepatic triglyceride lipase levels in hemodialysis patients. *Kidney Int Suppl* **71**: S213-215.
25. Bing, C. Lipid mobilization in cachexia: mechanisms and mediators. *Curr Opin Support Palliat Care* **5**: 356-360.
26. Fouladiun, M., U. Korner, I. Bosaeus, P. Daneryd, A. Hyltander, and K. G. Lundholm. 2005. Body composition and time course changes in regional distribution of fat and lean tissue in unselected cancer patients on palliative care--correlations with food intake, metabolism, exercise capacity, and hormones. *Cancer* **103**: 2189-2198.
27. Das, S. K., S. Eder, S. Schauer, C. Diwoky, H. Temmel, B. Guertl, G. Gorkiewicz, K. P. Tamilarasan, P. Kumari, M. Trauner, R. Zimmermann, P. Vesely, G. Haemmerle, R. Zechner, and G. Hoefler. 2011. Adipose triglyceride lipase contributes to cancer-associated cachexia. *Science* **333**: 233-238.
28. Swift, S., A. R. Ellison, P. Kassner, I. McCaffery, J. Rossi, A. M. Sinclair, C. G. Begley, and S. Elliott. Absence of functional EpoR expression in human tumor cell lines. *Blood* **115**: 4254-4263.



## FIGURE LEGENDS

### FIGURE 1

Representative patterns (lower) and densitometric analysis (upper) of EPOR (A) and phosphorylated (Ser473) and total Akt (B) expression measured in WAT protein extracts. C= control mice; LLC= Lewis lung carcinoma-bearing mice; EPO= erythropoietin administered. C. Lipoprotein lipase (LPL) enzymatic activity in WAT protein extracts. Data (means  $\pm$  SD) are expressed as percentages of controls. Significance of the differences: \*  $p < 0.05$  vs C; \*\*  $p < 0.01$  vs C; \$  $p < 0.05$  vs LLC.

### FIGURE 2

A. Lipogenic rate assayed on WAT fragments measuring the incorporation into lipids of [1-14C] acetate (see methods). B. Lipolytic rate assayed on WAT fragments measuring the glycerol release (see methods). C= WAT from control rat; AH-130 = WAT from AH-130 bearing rat. Data (means  $\pm$  SD) are expressed as percentages of controls. Significance of the differences: \*\*  $p < 0.01$  vs C; \*\*\*  $p < 0.001$  vs C; \$\$  $p < 0.01$  vs TNF; #  $p < 0.05$  vs AH-130.

### FIGURE 3

A. Phase contrast microscopy (upper images) and EPO receptor immunofluorescence (lower images; blue: nuclei) of 3T3-L1 adipocytes at early (4 days) differentiation stages. B. Lipid accumulation measured as Oil Red O uptake. C. mRNA levels of genes related to adipogenesis. Data (means  $\pm$  SD) are expressed as percentages of controls. Significance of the differences: \*  $p < 0.05$  vs C; \$  $p < 0.05$  vs TNF.

### FIGURE 4

A. Representative pattern of EPOR time-course expression during 3T3-L1 growth and differentiation. B. Growth curve in preadipocytes (Crystal violet staining, see Material and methods).

### FIGURE 5

Schematic drawing of EPO actions on the adipose tissue.

**Table 1.** Body and tissue weights of tumour-bearing mice.

**A. C26 tumour model**

	<b>CONTROL (7)</b>	<b>C26 (7)</b>	<b>C26+EPO (6)</b>
<b>IBW</b> (g)	25,30 ± 0,68	24,92 ± 0,55	24,52 ± 0,62
<b>FBW</b> (g)	26,98 ± 0,72	20,94 ± 0,86 ***	21,71 ± 0,85 ***
<b>Cumulative food intake</b> (g)	50,31	39,90	40,86
<b>Tumour</b> (mg/100 g IBW)		1563 ± 200	1602 ± 173
<b>Haematocrit</b> (%)	51,02 ± 0,80	42,80 ± 0,69 ***	47,98 ± 1,12 §§
<b>epididimal WAT</b> (mg/100g IBW)	608 ± 46	200 ± 30 **	346 ± 39 *§
<b>dorsal WAT</b> (mg/100g IBW)	407 ± 40	61 ± 15 ***	127 ± 22 *** §
<b>Gastrocnemius</b> (mg/100g IBW)	534 ± 13	409 ± 11 ***	439 ± 24 **
<b>Tibialis</b> (mg/100g IBW)	181 ± 3	136 ± 5 ***	143 ± 11 **

**B. LLC tumour model**

	<b>CONTROL (6)</b>	<b>LLC (7)</b>	<b>LLC+EPO (7)</b>
<b>IBW</b> (g)	19,23 ± 0,71	19,89 ± 0,19	19,98 ± 0,03
<b>FBW</b> (g)	20,84 ± 0,44	16,36 ± 0,50 ***	17,75 ± 0,25 ***§
<b>Tumour</b> (mg/100 g IBW)		5052 ± 150	4967 ± 375
<b>Cumulative food intake</b> (g)	44,27	38,12	37,85
<b>Haematocrit</b> (%)	59,09 ± 0,25	25,79 ± 0,55 ***	30,91 ± 0,59 ***§
<b>epididimal WAT</b> (mg/100g IBW)	1151 ± 62	145 ± 30 ***	307 ± 46 ***§
<b>dorsal WAT</b> (mg/100g IBW)	277 ± 34	14 ± 4 ***	42 ± 8 ***§§
<b>Gastrocnemius</b> (mg/100g IBW)	551 ± 16	390 ± 18 ***	417 ± 10 ***
<b>Tibialis</b> (mg/100g IBW)	189 ± 9	128 ± 6 ***	124 ± 3 ***

Results are mean ± S.E.M. for the number of animals indicated in parenthesis. Tissue weights are expressed as mg/100 g of initial body weight. Final body weight (FBW) excludes the tumour mass. IBW: Initial body weight, WAT: white adipose tissue. Statistical significances analysed using ANOVA.

Figure 1A

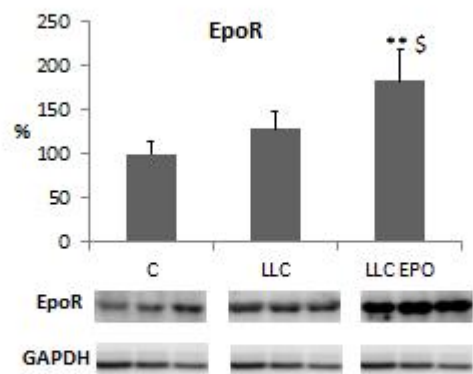


Figure 1B

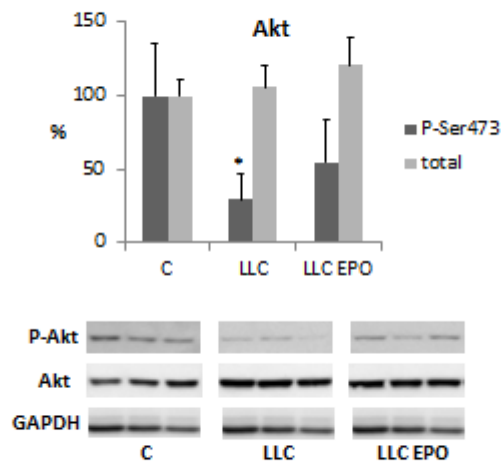




Figure 1C

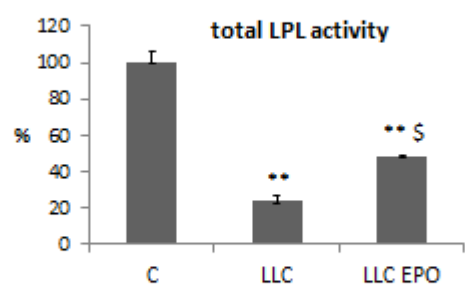


Figure 2A

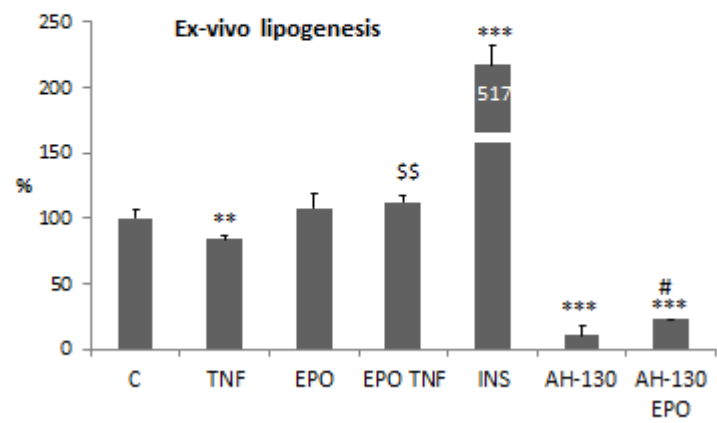


Figure 2B

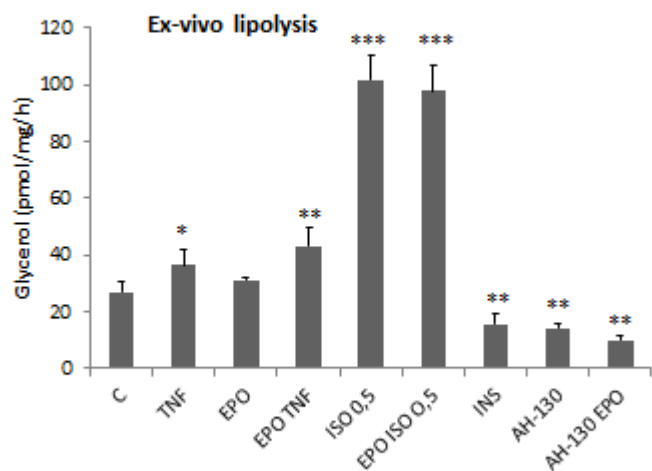


Figure 3A

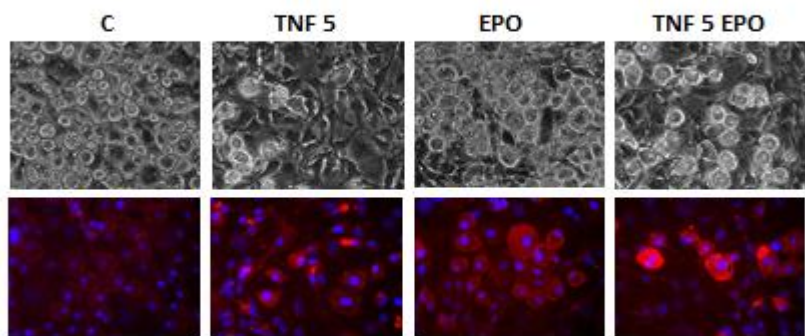


Figure 3B

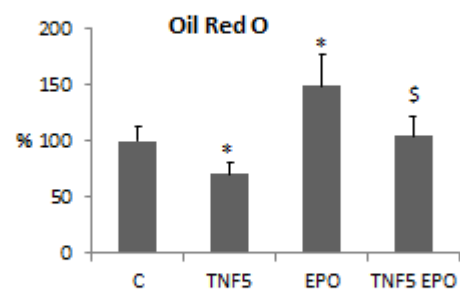


Figure 3C

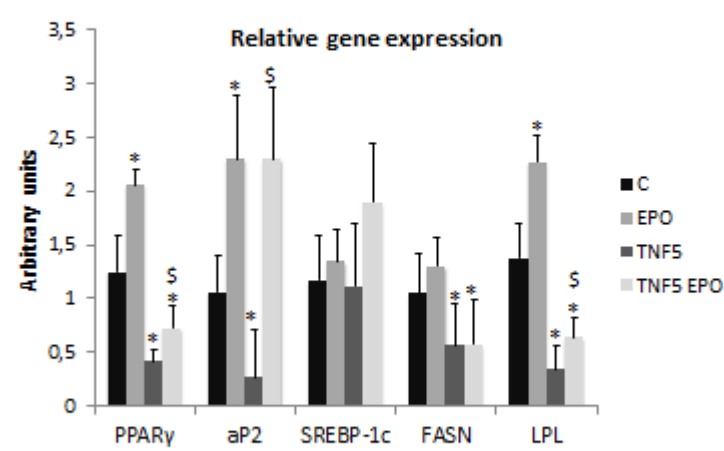


Figure 4A

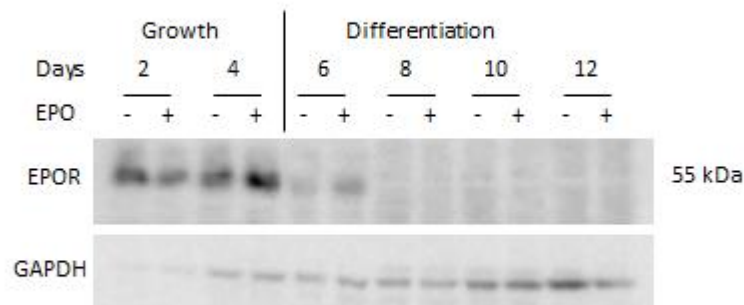


Figure 4B

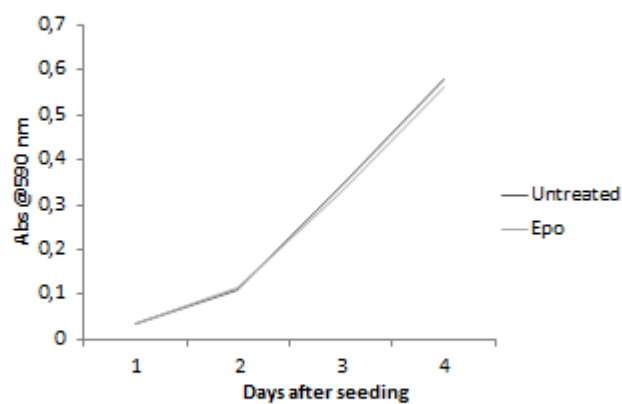


Figure 5

